

CONF-9004194-End

NOTICE

Chicago, IL 10-19

This is an advance copy of a paper to be presented to the Joint Railroad Conference of ASME/IEEE in April 1990. This copy is made available to selected persons, companies, and others who may be interested in advancement of the project. Portions may be reproduced for internal use and coordination with other interested parties, but permission to publish is withheld until presentation of the paper.

FINAL DRAFT

**VALIDATION OF "SYSTEM 21" MONOBÉAM TRANSIT
WITH COMPUTER ANALYSIS AND LARGE MODELS**

CONF-9004194--1

DE90 010046

L. K. Edwards, President, FUTREX inc
D. R. Ahlbeck, Manager, Dynamics Section, Battelle
P. B. S. Lissaman PhD, Vice President, AV Dynamics
W. J. Mouton, C.E., Professor, Tulane University
R. O. Powell PhD, Professor, Tulane University

FG 01-89C E15439

ABSTRACT

Validation of four key features of the new "SYSTEM 21" ¹ aerial rapid transit system are discussed:

- o Assessment of tension tie between car and beam by Mr. Ahlbeck.
- o Dynamic analysis of cars/trains traveling along the guideway at speeds to 100 mph, by Dr. Lissaman.
- o Analyses of guideway beam strength and rigidity by Dr. Powell and Prof. Mouton.
- o Quarter-scale models to validate outrigger kinematics and modular makeup of the guideway and station.

There are strong indications of suitability for operation at inter-city speeds as well. Most of this was done under a DOE grant to FUTREX in 1989, addressing issues identified by the National Bureau of Standards.

INTRODUCTION

SYSTEM 21 is a new form of monobeam rail rapid transit, optimized for placement above streets and boulevards in metropolitan areas. As will be shown, it also has the potential for inter-city applications at speeds of the order of 100-125 mph.

The system was discussed as "Project 21" in references 1 through 3. It employs cars the size of a small urban bus, with seats for 24 and standing space for another 24. Thus four-car trains can carry up to 192 passengers; at one-minute headways, this permits roughly 11,000 passengers per hour per direction, i.e., nearly the same peak-hour ridership as is experienced in any American city except New York (and well above any line in Boston, Philadelphia, or Atlanta).

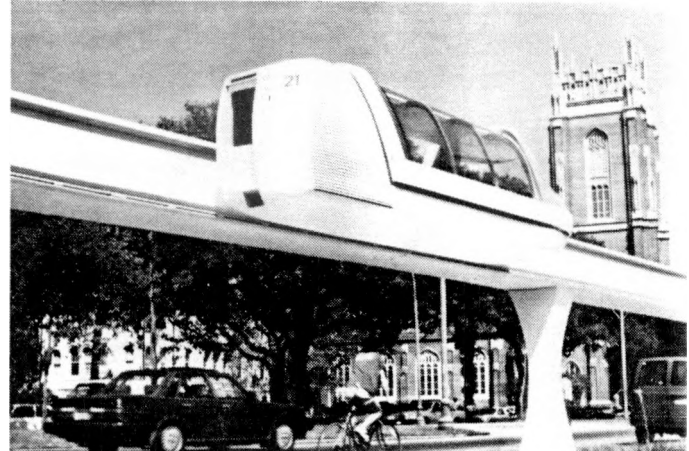


Fig 1. SYSTEM 21 along St. Charles Avenue (1/4-scale model).

Uniquely, the system uses a single beam or guideway for two-way traffic, with trains traveling along opposite sides of the beam. The generic term for this technology is "monobeam". Stations, too, serve two-way traffic for up to four-car trains; they have two stairways and a large elevator. Both the guideway and stations are configured for factory production in standardized modules, with installation at the jobsite within a week or two after the concrete footings are in place. The baseline guideway is a steel weldment, but concrete beams are also being studied.

Fig 1 shows how the system would look along St. Charles Avenue in New Orleans. These quarter-scale models were constructed by a class at Tulane University there. Fig 2 shows how the system would fit into a dense urban area, above a six-foot median in the center of the street.

The cars are electrically propelled with 600 VDC motors. Each car has two "trucks", each consisting of a motor, gearbox, and steel wheel as shown in fig 3. All propulsion and braking are via these lower wheels, which engage a conventional (but inclined) 90-pound steel rail that is fastened to the beam. To prevent overturning, there is an "outrigger" above each truck.

¹ "SYSTEM 21" and "FUTREX" are registered marks of FUTREX inc. Many features of the system described here are covered by U.S. Patent 3,890,904

DISCLAIMER

This report was prepared as an account of work sponsored by an agency of the United States Government. Neither the United States Government nor any agency thereof, nor any of their employees, makes any warranty, express or implied, or assumes any legal liability or responsibility for the accuracy, completeness, or usefulness of any information, apparatus, product, or process disclosed, or represents that its use would not infringe privately owned rights. Reference herein to any specific commercial product, process, or service by trade name, trademark, manufacturer, or otherwise does not necessarily constitute or imply its endorsement, recommendation, or favoring by the United States Government or any agency thereof. The views and opinions of authors expressed herein do not necessarily state or reflect those of the United States Government or any agency thereof.

DISCLAIMER

Portions of this document may be illegible in electronic image products. Images are produced from the best available original document.



Fig 2. Above a 90-foot street in dense urban area (model).

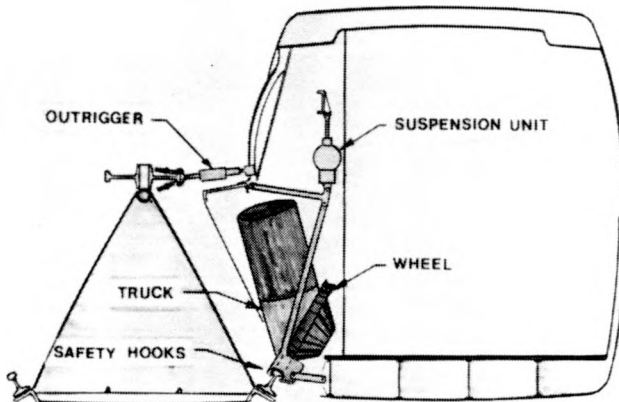


Fig 3. Section through car at outrigger (typical 2 places).

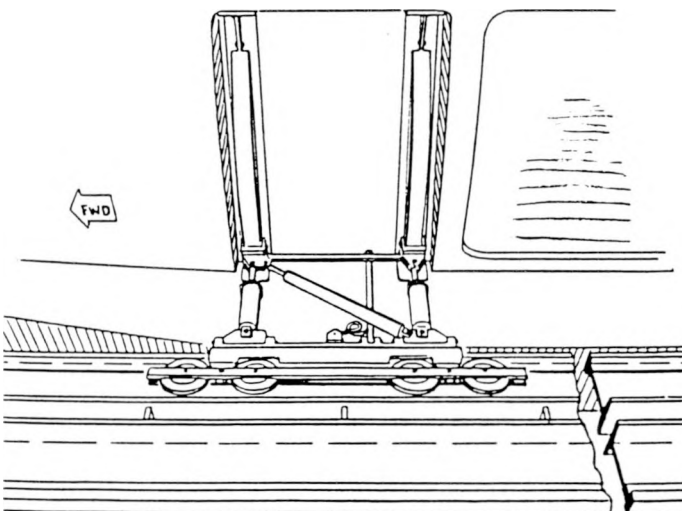


Fig 4. View of outrigger looking toward car.

Each outrigger has a group of eight rollers that engage a special upper rail. As shown in figs 3 and 4, the rollers ride on the inner flange of the railhead. Thus the car/train imposes both bending and torsional loads on the beam.

At stations, the upper rail is placed above the passageway doors as shown in fig 5. This requires that the outrigger "swing up" relative to the car as it approaches a station; this is accomplished by a progressively deepening guideway beam adjacent to the station (fig 5) and by incorporating a movable attachment between the outrigger and the car structure (fig 6).

This paper presents results of a preliminary assessment of the above features by FUTREX and four subcontractors, sponsored by the Department of Energy under a Grant identified as DE-FG01-89CE15439.

Results of the individual studies/assessments will be presented in the following sequence:

1. Strength and rigidity of the guideway beams for spans of 75 to 99 feet, by Dr. Powell and Prof. Mouton.
2. Dynamics of the ride over spans from 75 to 99 feet at speeds of 55 to 100 mph, by Dr. Lissaman.
3. Integrity of the outrigger per se, by Mr. Ahlbeck.
4. Model of the modular station and approach beam, by Prof. Mouton.

System parameters used in all of the analyses included the following:

Car length/wheelbase	28 feet/18 feet
Empty weight	11,000 pounds
Crush-loaded weight	17,500 pounds
Car C.G. - offset from center of beam	64.5 inches
Lower rail slope	30° from vertical
Outrigger slope (except in stations)	5° from horizontal

0.5 g earthquake with a crush-loaded train on one side
 0.3 g earthquake with normal-loaded trains on both sides
 40 psf winds (approx 120 mph) with a train on the beam
 60 psf winds (approx 150 mph) on the beam alone.

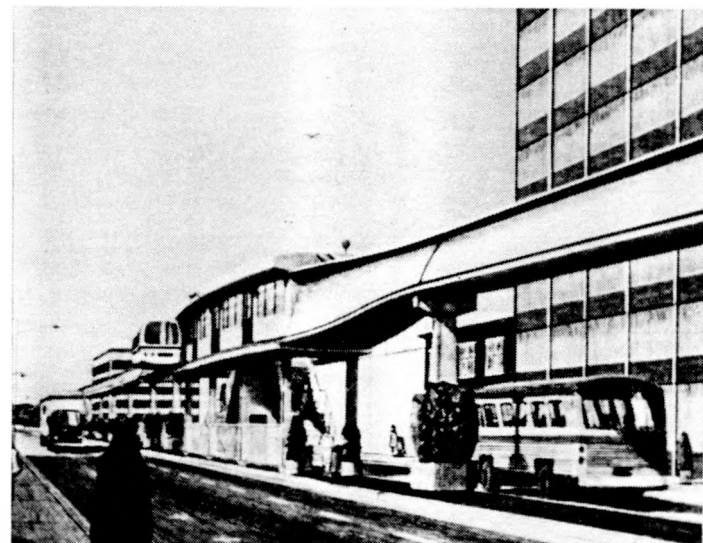


Fig 5. Perspective of station showing approach beam.

There is no bending continuity from beam to beam, but there is torsional continuity.

Note that a four-car train is longer than a 99-foot beam; in fact, the distance from the first wheel to the last wheel is 102 feet. Thus the beam designs should be good for much longer trains, as needed. (However, columns and footings could be affected).

Before discussing the results of individual analyses, one should understand (1) the effect of beam torsion on the car's behavior, and (2) the effect of pre-camber.

When a car or train travels along a monobeam, its vertical and rotational positions are slaved to the beam deflection and twist. At midspan the car will settle with the beam, but will experience additional settlement (and rotation) as the beam twists. A fully-loaded 4-car train will see greater deflection/twist than a single car with only a few passengers.

It is customary in bridge design to incorporate "pre-camber" in each span to anticipate not only the deflections due to structural deadweight but also a moderate allowance for the "live load." Then a small automobile would experience a slight hump between supports and a dump truck would feel a slight dip. The pre-camber is necessarily a compromise that reflects the range of live loads.

In monobeam design these considerations apply, but additional allowance is made in the pre-camber to compensate for the beam twist. These considerations can be combined by focusing on the effective deflection in the passenger space of the car, referred to here as the car "CG," some 64.5 inches from the beam centerline.

Now consider what happens when two trains pass each other on the beam. While the bending deflection increases, the twist drops to zero. Thus the total deflection, as seen in either train, changes surprisingly little.

Now we present the results of the individual analyses.

BEAM STRENGTH AND RIGIDITY

Finite Element Analysis (FEA) was performed on the steel beam structure as defined by Edwards and Mouton, with an I of 51,000 in⁴, and a prestressed concrete beam as defined by Mouton with an equivalent I of 67,250 in⁴. The main focus was on 75-foot spans. The defined structure had its supports one foot from the beam end; hence, the clear span for analysis was 73 feet.

The FEA was for vertical loads only and used sections as shown in fig 7. Due to spanwise symmetry it was sufficient to model only half of the 73-foot span; i.e. a 36.5-foot span. There were 21 station cuts, for a total of 189 nodes.

In both structures there is 26.5 in² of steel to account for the two upper rails and their connection to the webs; this was effectively treated as a simple chord with negligible (local) moment of inertia. Similarly, at each lower corner there is 15.8 in² of steel to account for the 90-pound-per-yard rail and its attachment to the webs.

Web thicknesses are $\frac{1}{4}$ " for steel and 4" for concrete, with some additional "beef" at the beam-end and an allowance of 84 pounds/ft for electrical and other non-structural features. All-up dead weight for the steel beam is 36,000 pounds, as compared to 72,000 for concrete.

Fig 8 is a sample printout of the FEA for a 75-foot steel beam, before consideration of pre-camber; the tabulated results of that case are:

	Comp stress at top (psi)	Tensile stress at bottom (psi)	Deflection at car CG
Beam deadweight	2202	1477	(.20)*
DW+1 car @ 14K	3539	2374	.38
DW+4 cars/1 side	5148	3453	.61
DW+4 cars/2 sides	8093	5427	.72

(*Denotes value for a weightless car)

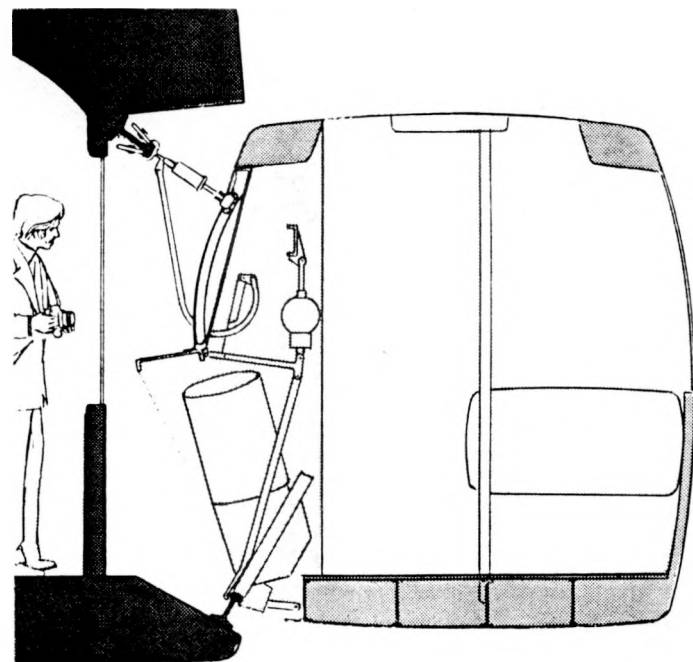


Fig 6. Section through car and rails at station (outrigger raised).

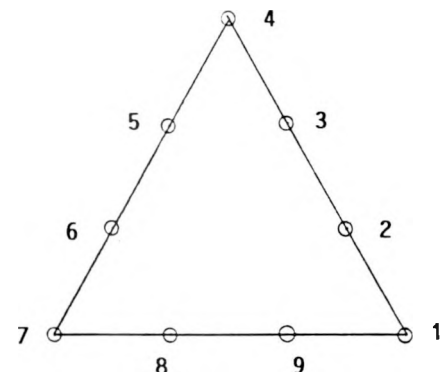


Fig 7. Identification of nodes for Finite-Element Analysis

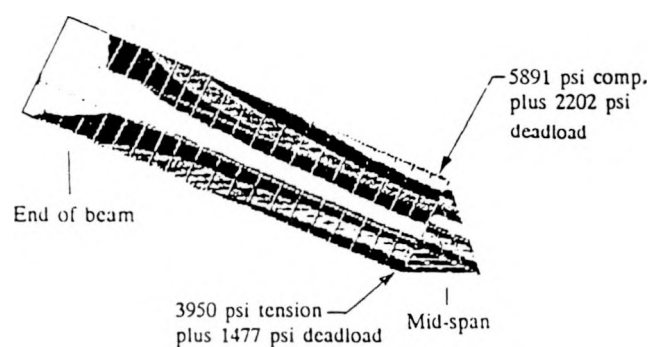


Fig 8. Live-load stresses with crush-loaded trains on both sides of a 75-foot beam.

The above stresses are characterized as "less than half the working stresses allowed by AISC." However, the deflections can be improved, without affecting the stresses.

Consider the effect of a judicious pre-camber of .53 total, or .33 in addition to that needed to offset the deadload deflection:

<u>Condition</u>	<u>Between columns</u>	<u>Variation from straight path</u>
one car	.15 humps	$\pm .07"$
4 cars one side	.08 dips	$\pm .04"$
4 cars 2 sides	.19 dip	$-.15"$

FEA results for 75-foot concrete beams before allowance for prestressing and camber are:

	<u>Comp stress at top (psi)</u>	<u>Tensile stress at bottom (psi)</u>	<u>Deflection at car CG</u>
Beam deadweight	618	374	(.36)*
DW+1 car @ 14K	804	486	.49
DW+4 cars 1 side	1026	621	.66
DW+4 cars 2 sides	1434	867	.82

(*Denotes value for a weightless car)

In light of these results we plan to incorporate prestressing and camber as follows:

- o Prestressing to assure compression throughout the concrete in all conditions.
- o Camber of .60 nominal before deadload or .24 after deadload.

Now the FEA results for the 75-foot concrete beam become:

	<u>Comp stress at top (psi)</u>	<u>Comp stress at bottom (psi)</u>	<u>Between columns (in.)</u>	<u>Variation from straight path (in.)</u>
DW+1 car	1074	1364	.11 humps	$\pm .055$
DW+4 car (1 side)	1296	1229	.06 dips	$\pm .03$
DW+4 car (2 sides)	1704	983	.22 dip	.19 dip

Allowable compressive stresses for the concrete are 3600 psi, so margins are generous.

Beam twist in the above analyses has been taken into account when presenting the "deflection at car CG". The absolute amount of twist, at worst, is only .13 degrees for the steel beam and .29 degrees for concrete. We will consider fine-tuning the placement of the rail so that the car floor does not rotate through this small range as it traverses the span.

All of the above is based on static deflections. Will dynamic deflections be significantly more? The next section of this paper indicates that they will not.

The FEA confirms earlier calculations based on simple beam theory. Similar calculations have also been performed on transverse loading conditions (earthquake and wind), with results as in Table 1. The use of 8-car trains in this instance brings out the loads and stresses that would be incurred for unlimited train lengths. Wind values of 60 psf are equivalent to approximately 150 mph winds. Note that in this and in the preceding analysis, adequate strength margins are obtained with beam spans up to 99 ft (both steel and concrete); however, as deflections tend to increase with the cube of the span, it remains to be determined whether spans of that length should be chosen for general use. The logistics of delivering and erecting such long spans must also be considered.

Table 1. Summary of Lateral Loads on Beams and Columns.

SYSTEM 21: SUMMARY OF LATERAL LOAD ANALYSIS										WJM
LOADS:	CRUSH LOADS: 17,500# CARS									16 JAN '90
COLUMNS:	18 FEET CLEAR HEIGHT									
	8 CAR TRAINS									
	(+ = Tension)									
	(- = Compression)									
SPANS:	SEVENTY FIVE FEET (75'-0")									
LOADING:	Earthquake	Wind	STEEL BEAM	STEEL COLUMN	P/S CONCRETE BM	P/S CONCRETE COLUMN				
			Left Side	Rt. Side	Left Side	Rt. Side	Left Side	Rt. Side	Left Side	Rt. Side
TRAIN 1 SIDE	.5G	0	0.51	6.40	16.45	-17.71	-1.71	-0.75	0.58	-3.10
TRAIN 2 SIDES	.3G	0	2.58	8.27	11.56	-13.50	-1.39	-0.58	-0.02	-2.58
TRAIN 1 SIDE	0	60 psf	0.70	6.21	15.68	-17.62	-1.53	-0.93	0.13	-2.65
TRAIN 2 SIDES	0	40	3.59	7.27	7.37	-9.30	-1.18	-0.78	-0.61	-0.99
Allowable Stresses:			31.92	31.92	31.92	-26.60	-4.79	(+) 0.71	(+) 0.71	-4.79
Minimum Factor of Safety			9.96	4.32	2.17	1.68	4.20	3.20	1.84	2.32
SPANS:	NINETY-NINE FEET (99'-0")									
LOADING:	Earthquake	Wind	STEEL BEAM	STEEL COLUMN	P/S CONCRETE BM	P/S CONCRETE COLUMN				
			Left Side	Rt. Side	Left Side	Rt. Side	Left Side	Rt. Side	Left Side	Rt. Side
TRAIN 1 SIDE	5G	0	-1.75	8.65	20.4	-22.02	-2.07	-0.39	0.65	-3.01
TRAIN 2 SIDES	3G	0	0.41	10.45	14.07	-16.58	-1.69	-0.27	0.04	-2.51
TRAIN 1 SIDE	0	60	-1.42	8.32	19.58	-22.09	-1.76	-0.7	0.21	-2.57
TRAIN 2 SIDES	0	40	2.18	8.67	8.98	-11.50	-1.34	-0.63	-0.55	-1.92
Allowable Stresses:			-26.60	31.92	31.92	-26.60	-4.79	(+) 0.71	(+) 0.71	-4.79
Minimum Factor of Safety			17.02	3.42	1.75	1.35	3.47	2.07	1.64	2.39

DYNAMIC ANALYSIS

The objective of the dynamic analysis was to assess the ride dynamics for various size trains traveling along guideways with given torsional and flexural rigidity and spans from 75 to 99 feet.

Modeling procedures

Two mathematical techniques were used, the first being an exact analytical solution for a spanwise uniform beam for both a moving point load and a moving distributed load, both without eccentricity.

The first procedure is a purely analytical approach which provides an exact solution, in terms of a Fourier expansion, to a somewhat idealized case, treating the restricted case of a beam with spanwise uniform mass and stiffness traversed by a single concentrated load moving across it at uniform speed. An extension of this solution solves the case of a uniformly distributed load moving at uniform speed across the span. Because of the omission of eccentricity and relatively simple nature of the parameters, exact solutions for these cases can be developed and expressed as a rapidly convergent Fourier Series.

The second procedure was to use a Finite Difference Model (FDM) in which the detailed geometry of the structure was treated and the car suspension and unsprung mass were modeled as a multi-degree of freedom system so that the discrete loads were applied in a dynamically correct fashion. The solution was obtained by integrating the acceleration with respect to time and distance.

In the FDM the structure is divided into a number of small elements and the primitive beam and Newton equations are solved directly in the time domain as the car moves over the span. This method permits us to incorporate eccentric loading, arbitrary spanwise mass and structural properties of the beam, the suspension arrangements of the car, and the speed of traversing the span as well as the effect of traversing multiple spans and the effect of pre-camber and irregularities in the guideway profile. The analytical method already described is particularly useful for obtaining rapid results and also for checking the accuracy and convergence of the FDM, by testing it against the exact solution for the simple case.

The analytic solution defines a resonant speed which occurs when the load crosses the span in one half the natural period of the unloaded beam. Because of the time dependent nature of the numerator the resonant case does not cause a divergence in the deflection, as would occur for a long term oscillatory load at this frequency, but results in a finite deflection and bending moment, having a maximum near the midspan, and having a magnitude of about 150% of their values for the case of a static load located at the midspan. This is a useful rule of thumb, and consistent with other well-known results; for example, the case when the load is suddenly applied at the midspan, i.e. the classical suddenly applied load, where the bending moments and deflections are 200% of the static case.

For the parameters of the guideway the resonant time for passage is about 0.06 seconds, which would correspond to a vehicle speed in excess of 800 mph, indicating that the system is very far from resonance and that even the 50% amplification over static conditions will not occur.

This point is illustrated by fig 9 which shows the guideway deflection under the load for the static case (0 mph) and the case of 75 mph. It is noted that the dynamic deflection amplification is very small.

The Finite Difference Model was written in such a form that many of the structural parameters could be arbitrarily varied. For this model the beam is represented by a beam of spanwise variable properties, having vertical flexural deflection as well as the torsional deformation which is occasioned by the off-set of the car center of

gravity from the torsional center of the beam. The pre-camber of the beam was arbitrary. The flexural stiffness is represented by the equation:

$$EI y'''' = sl$$

Where EI represents the structural rigidity, y'''' the fourth spanwise derivative of vertical deflection and sl the spanwise loading per unit length. The torsional stiffness is represented by:

$$GJ \phi'' = st$$

where GJ represents the torsional rigidity, ϕ'' the second spanwise derivative of the twist and st is the spanwise torsion per unit length. The torsional rigidity, GJ , was calculated using Bredt's formula for the twist of a closed thin-walled member and the end constraints for torsion were taken as fixed, that is without rotation. The car was assumed supported by a suspension system in the front and rear by trucks, each of the same stiffness. An arbitrary car pitch moment of inertia and unsprung suspension mass was modeled. The spring stiffness was initially taken to give the natural vibration of the car on a rigid guideway of 1 Hz, which is representative of light rail suspension systems. The solution was derived for no suspension damping, but was implemented so that a deflection-rate-dependent damping could be inserted. The code also has the capability to vary the truck suspension parameters.

Finite difference representations were written for the beam for motion due both to vertical deflection and torsion and for the displacement of the car at its forward and rear trucks and the resulting equations solved directly in the time domain. This makes it possible for the car to enter each span with the motion corresponding to that with which it left the previous span, so that the motion over multiple spans may be calculated. The model also handles the case of a multiple-car train, where successive cars are connected by a coupling that transmits only traction and thus does not permit any shear, torsional or flexural constraint between cars.

Basic Structural Results

Basic structural loads and deflections were calculated for the system for the appropriate parameters. For the static case with a single car at the center of the span, the flexural bending stress was about 4,100 psi, the additional deflection due to the car is 0.19 inches over that of the track alone, and the torsional deflection 0.07 degrees. For the four car train the corresponding figures at the center of the span were 5,900 psi, 0.38 inches additional deflection, and 0.13 degrees. These calculations are made for a span of 80 ft. If the 99 ft span is assumed, then for the four-car train the

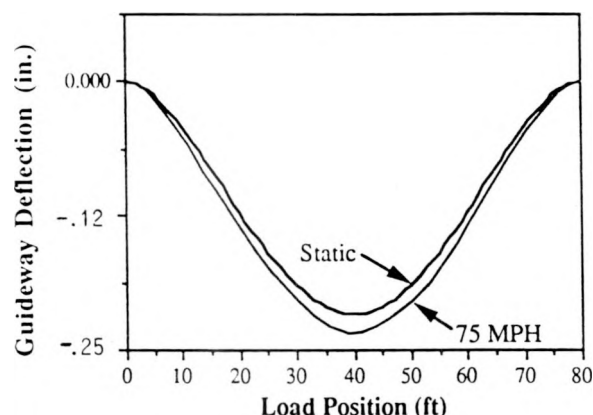


Fig 9. Guideway deflection vs load position for 0 to 75 mph.

maximum static flexural bending stress is about 8,900 psi, the additional deflection is 0.87 inches, and the torsional deflection, 0.19 degrees. The table below gives the complete results for the cases considered; these values are reasonably consistent with the finite-element-analysis results given earlier, when allowance is made for the longer spans assumed here.

Case	Stress (psi)	Vertical Deflection (in.)	Beam Rotation (deg)	Total deflection at car lateral CG (in.)
80' beam (alone)	2085	0.16	0.00	0.16
80' beam (1 car)	4105	0.35	0.07	0.44
80' beam (4 cars)	5925	0.54	0.13	0.69
99' beam (alone)	3193	0.38	0.00	0.38
99' track (4 cars)	8894	1.25	0.19	1.45

The stress is given at the beam center, where it is maximum. Deflections and rotations are given at the wheel closest to the beam center. The total deflection at the car is given at the wheel nearest beam center and at the car lateral CG. Car placement is symmetric about center span. All of these values are totals, including effects of all the loads.

For the unloaded beam the various natural frequencies were calculated. The flexural vibration of the beam occurred at frequencies of 7.8 Hz and 31.1 Hz for the first two modes, while the

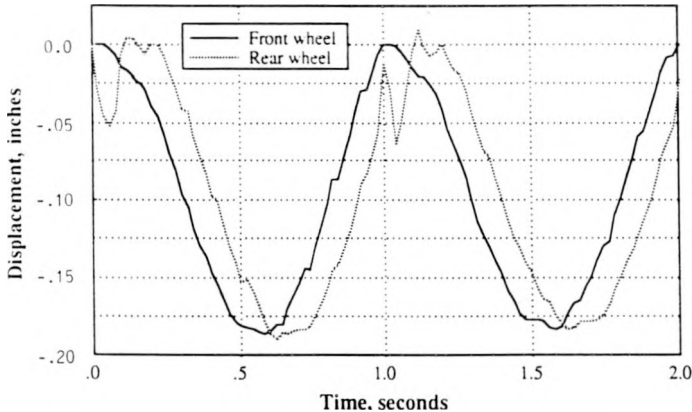


Fig 10. Trajectory of wheels/trucks at 55 mph before pre-camber.

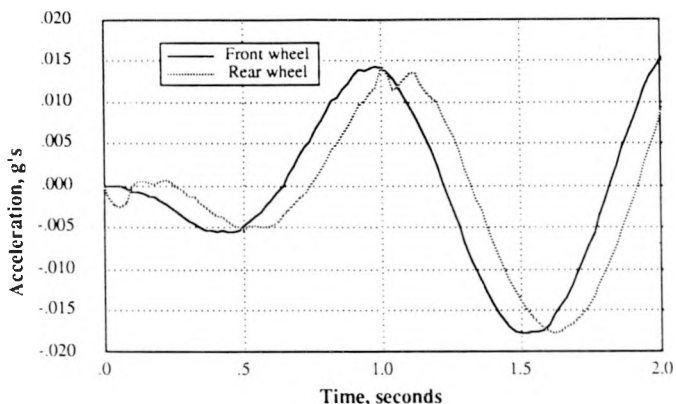


Fig 11. Accelerations at car CG before pre-camber.

first two torsional modes were at 26.3 Hz and 52.5 Hz. Separation of these frequencies is adequate to avoid dynamic interactions.

Finite Difference Model Dynamics

The FDM was used to find the trajectories and accelerations of a car. The cases considered are for the standard system parameters with a single car at a speed of 55 MPH on a span of length 80 feet. This gives a span traverse time of about 1 second. It is noted that this time of passage is very slow compared to the resonant time of the beam which, as shown above is about 0.06 secs. Cases with a flat track and a pre-cambered track are presented. For all cases the simulation is done for a total of two seconds, about the time it takes the vehicle to traverse two spans. The effects of suspension damping are not included.

A simulation begins with the front wheels of the car directly above a column. The car is then moved forward in small time increments, with the equations of motion being solved for the track flexural and torsional deflection coupled to the vehicle sprung mass and the unsprung mass.

In the case of the beam, 40 elements were used to define its shape. In order to solve the equations for this model, the time step was required to be 0.001 of the time it takes the car to traverse one element. This corresponds to about 25 micro seconds (25×10^{-6} secs). These small time steps are needed to resolve the highest mode of the beam oscillations. Even with this short time step, the highest mode cycles take place in only about ten time steps. To traverse an entire span thus takes 40,000 time steps. This requires about one hour of run time on the computer.

The first case calculated is for a single car and a flat track; that is, with only that pre-camber needed to account for dead load. Fig 10 shows the track vertical deflection at each wheel. The wheels follow similar trajectories, with the rear wheels lagging about 0.1 second behind the front wheels. This lag is less than the actual of 0.2 seconds that it takes the car to traverse a distance equal to the wheel base. The difference in the lag times is a result of the dynamic beam deformation under the weight of the car indicating good fidelity in the model solution.

It will be noted that the peak deflection is approximately 0.18 inches. The small jumps and kinks in the plot are artifacts of the numerical method used to solve the equations. It is noted that the deflection is of the same order as that found by the analytical calculation which gave a value of less than 0.20 inches. The very close correspondence of the two results indicated that the time steps taken in the FDM were sufficiently small to yield a suitably convergent numerical result.

For the car and the passengers, the ride quality can be assessed from the vehicle vertical accelerations. This is shown in fig 11. Accelerations in the car directly above the front and rear trucks are shown in the figure. It is noted that the maximum acceleration

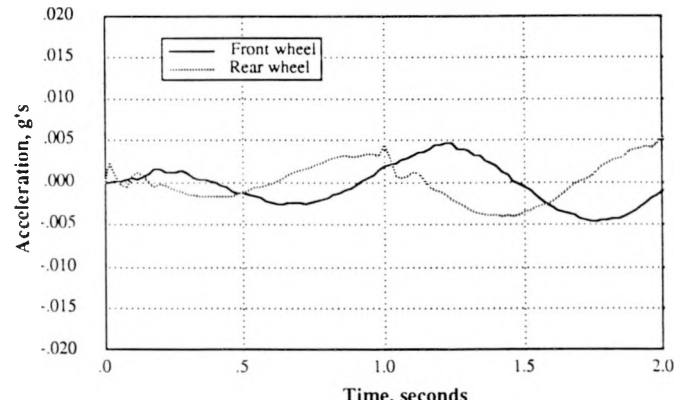


Fig 12. Accelerations at car CG after pre-camber.

is about 0.017 g. The natural period of the vehicle oscillation on its suspension is about one second, and from the figure it can be seen that about two cycles have taken place. It is noted that the car natural frequency is thus about the same as the span crossing frequency and since no suspension damping was used in the model, a slow divergence is to be expected. This indicates that the FDM is properly treating the dynamics. Model runs for longer time periods show that these oscillations do not grow rapidly, and in fact the peak accelerations seen in the long runs are not substantially greater than shown here. This mild response even without damping indicates that there should be no difficulty in controlling the motion with quite small suspension damping.

The acceleration can be reduced by further pre-cambering the track to cause the live load to follow a nearly horizontal trajectory. However, the front and rear wheels follow slightly different paths, and there will be many different train load cases, from empty single cars to fully loaded trains.

As noted earlier, pre-camber involves a compromise that reflects the range of live loads. Several values of pre-camber were explored; one valuable result was that train speed has almost no effect on the pre-camber choice. A representative pre-camber resulted in the car accelerations shown in fig 12. Pre-camber has reduced the car accelerations by a factor of 3 to 0.005 g -- a value barely perceptible to passengers.

Conclusions

1. This preliminary dynamic analysis indicates a very smooth ride with 80-foot steel beams at 55 mph, even without damping in the car suspension. The analytical tools will permit assessment of various spans, section properties, speeds, random anomalies, and suspension parameters.
2. It appears that, with suitable springing and damping, SYSTEM 21 can provide a smooth ride at 125 mph or more and with steel or concrete spans well over 80 ft.
3. The analysis should be extended soon to cover transverse effects, including winds and earthquakes. This should include the flexibility of columns and foundations.

OUTRIGGER ANALYSIS

The supporting outrigger is a key element in the safe operation of the SYSTEM 21 transit vehicle. This outrigger is subject not only to the quasi-static overturning load of the supported car and passengers, but also to dynamic loads in operation. These loads can be induced from several sources, including (1) guideway geometry errors, (2) guideway differential deflections under load at speed, (3) curving loads due both to centrifugal forces and to wheel/rail curving contact forces, and (4) externally-imposed forces, such as wind gusts and earthquake-induced loads. The possibility of high-speed "hunting" instability-induced forces must also be investigated soon.

One of the more difficult tasks in the early stages of a vehicle system design is to establish a realistic, yet conservative load environment for component safety and life assessment. There are examples in recent rail and road vehicle design where the dynamic load environment was grossly underestimated; resulting component failures in service caused substantial losses for both the manufacturers and the operating authorities. The development of a realistic load environment therefore becomes a key element in the success of the overall project. Our preliminary design evaluation was therefore focused on the types and magnitudes of dynamic loads to which the outrigger and suspension will be subjected, and the effects of these loads on the outrigger structural elements.

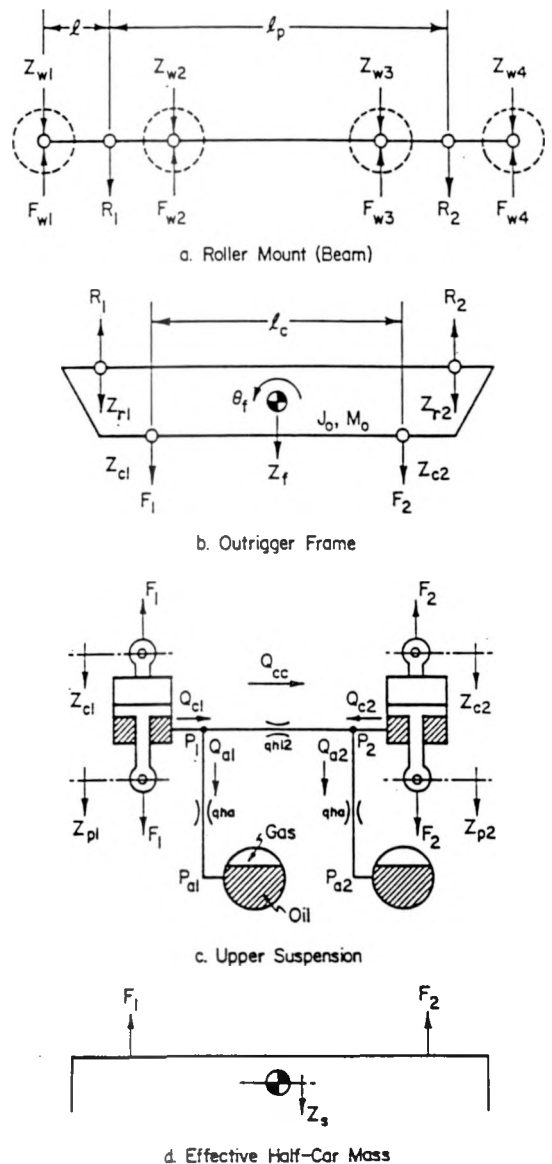


Fig 13. Elements of SYSTEM 21 outrigger mathematical model.

A mathematical model of the SYSTEM 21 outrigger was developed to define the operating load environment. Elements of this mathematical model are shown in fig 13. The model was programmed in FORTRAN 77 for time domain solution, and was configured for solution on the IBM compatible AT personal computer, giving a time-step printout of response variables and/or a summary table of maximum and minimum response values. Three variations of the program were generated: (1) response of a single detailed outrigger assembly and half-car body responding to typical rail geometry errors; (2) the leading (detailed) outrigger and half-car body entering a curve through a standard AREA cubic spiral, with the imposed geometry constraints from the rear outrigger and truck on the 18 ft spacing; and (3) two simplified outriggers (a single mass and stiffness, each) on the 18 ft spacing, and the whole car body in lateral and yaw, entering a curve through a standard AREA cubic spiral.

Four diverse track geometry-based loading conditions were used to investigate the SYSTEM 21 outrigger load environment. These included mismatched rails at a joint (a step up or down), a versine dip in the rail, a misaligned beam, and spiral/curve

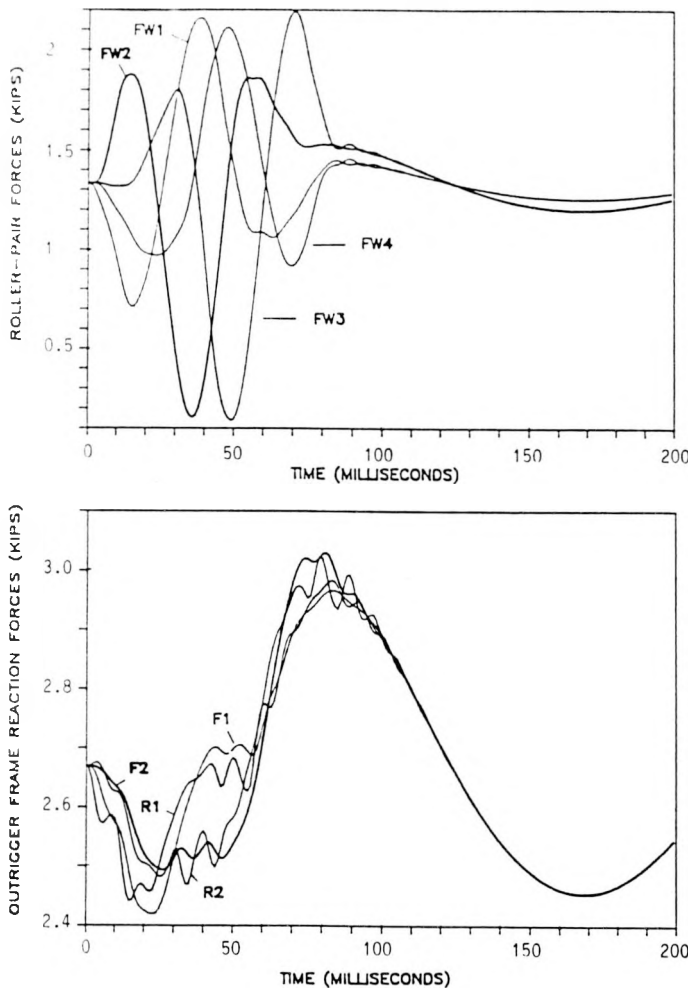


Fig 14. Typical outrigger time-history load response to 0.08-inch rail dip on 39.4-inch wavelength.

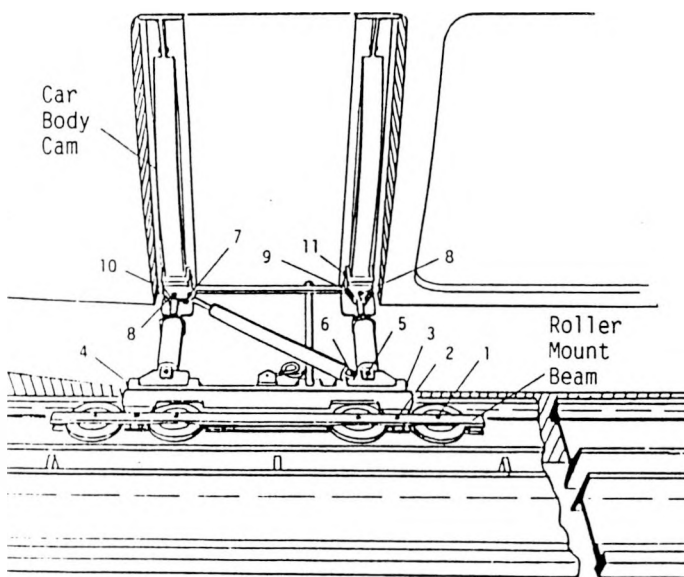


Fig 15. Outrigger joints numbered here were examined.

negotiation dynamics. Maximum and minimum loads at the key locations in the outrigger assembly were determined by use of the model. An example of predicted loads is given in fig 14, in which the outrigger rollers negotiate a 0.0788 inch dip on a 39.4 inch wavelength. Note that the roller-pair forces tend to decrease at first as each roller pair enters the dip. The trailing adjacent roller pair momentarily picks up the load shed by the pair ahead.

Using the computer model, the effects of several key parameters were investigated. These included the upper suspension gas volumes, guideway geometry error type and size, train speed, roller-mount beam compliance, system damping, and curve response. Computer results were used to predict the maximum loads at the principal outrigger and suspension elements. Based on these loads, a preliminary stress analysis was completed to assess the outrigger design integrity.

From these predictions, outrigger components must be designed to withstand dynamic and short-duration quasi-static overloads up to 2.5 times the static value at the rollers, up to 1.6 times static at the roller-mount-to-frame joints, and up to 1.4 times static at the upper suspension units. These loads were employed in a preliminary check of the 11 joints identified in fig 15, as well as stresses in key members. All appears to be satisfactory, although fatigue life of the roller-mount beam will require continued attention. (This mount is designed with sufficient resilience to conform to curves of ± 90 ft radius.)

The outrigger design maintains a basic redundancy throughout, so that mechanical failure (fracture) of a joint component will not result in loss of support of the car. Of course, a more detailed stress analysis is needed in the final design stages of the project; this detailed analysis would account for local stress concentration factors and would provide fatigue life assessment of components subjected to a statistically defined load environment.

After addition of gas-oil dampers as shown in fig 13, no significant problems were found, and it is concluded that outrigger integrity can be assured in the final detailed design. It would be prudent to conduct a similar analysis at the truck suspension and wheel-to-rail interface at an early date.

LARGE MODELS

In 1988-89, Mouton and his class at Tulane built, with FUTREX support, the quarter-scale model of the car and guideway illustrated earlier in fig 1. It had a simplified representation of the car suspension, including outrigger, to validate the fundamentals.

Under the DOE grant the car model has been refined to permit its outriggers to "swing up" as it approaches a station. More importantly, a complete half-station has been modeled so that the existing car can traverse the approach beam and illustrate the overall kinematics. The model also illustrates the modular breakdown that enables the station to be built in a factory and erected in 1-2 weeks. The overall design is shown in fig 16.

Status as of March 1, 1990 is shown in fig 17. Yet to be completed were the sliding doors, covering for the far wall and roof, the elevator, the approach beams, and the protective fence on the lower level. Rails to support the train are easily seen. Also evident in fig 17 is the structural framework, designed for easy fabrication from 3-inch-square steel tubing. The support columns are to be of concrete, trucked to the job for quick installation on ground-level footings.

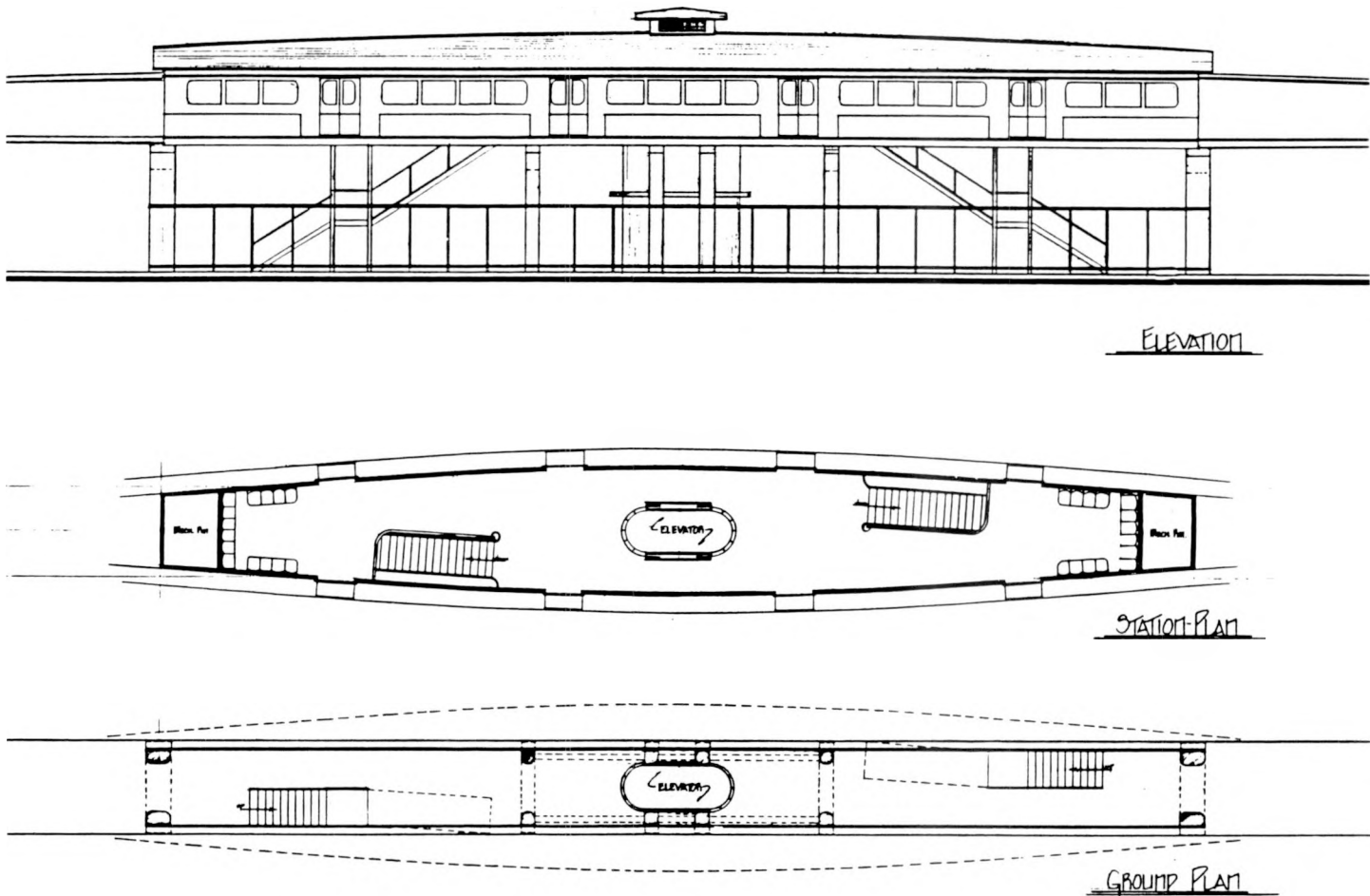


Fig 16. Baseline station design.

SUMMARY

These analyses have shown that the SYSTEM 21 designs are valid for beam spans to 80 ft and speeds to 60 mph. There are strong indications that spans can be increased to the order of 90 ft (if not 99 ft) and that speeds in the order of 125 mph are attainable with the same design, depending on precision of the joint from beam to beam and adaptability of the outrigger rollers for higher rotational speeds. The analytical tools for investigating these parameters are in place and validated.

The subjects investigated were highlighted in an earlier critique of SYSTEM 21 by the National Bureau of Standards (now NIST), reference 5.

It is concluded that:

1. SYSTEM 21 designs are suitable for the initial intent, i.e. rail rapid transit in metropolitan areas at speeds to 60 mph.
2. The potential of the same basic design to operate at intercity speeds is a pleasant surprise, and should be investigated further.

Copies of the individual analyses (references 5 through 7) are available from FUTREX inc. at nominal charge.

CONVERSION FACTORS

1 inch =	25.40 mm	1 mph =	1.609 km/h
1 foot =	0.3048 meter	1 fps =	0.3048 m/s
1 mile =	1.609 km	1 lb. m =	0.4536 kg
1 ksi =	1,000 pounds/in ²	1 kip =	1,000 pounds

REFERENCES

1. Edwards, L. K., "Project 21: A Practical New Intermediate-Capacity Rapid Transit System," Transportation Research Record 817, 1981, Transportation Research Board, National Research Council, Washington.
2. Edwards, L. K., "Project 21 Truck, Car-to-Guideway Interface, and Power/Performance," ASME Preprint 82-RT-9, Contributed by Rail Transportation Division of ASME.
3. Edwards, L. K., "Project 21: What's It All About?," 1988, FUTREX inc, Fairfax Va., (Presentation before National Rapid Transit Conference of APTA)
4. McGuire, B., "Recommendation No. 439: Project 21 Rapid Transit System," 1988, National Institute of Standards and Technology, Gaithersburg MD.
5. Mouton, W. J. and R. O. Powell, "SYSTEM 21 Guideway Analysis and Quarter-Scale Models," 1990, FUTREX inc, Fairfax VA.
6. Lissaman, P. B. S. et al, "Preliminary Dynamic Analysis of SYSTEM 21 Guideway and Vehicle Interaction", 1989, AV Dynamics, Monrovia CA.
7. Ahlbeck, D. R., "Preliminary Assessment of 'SYSTEM 21' Outrigger Design Integrity", 1989, Battelle, Columbus OH.



Fig 17. Quarter-scale station model as of March 1, 1990.